ELSEVIER

Chemical Geology 227 (2006) 53–69

CHEMICAL GEOLOGY
INCLUDING
ISOTOPE GEOSCIENCE

www.elsevier.com/locate/chemgeo

Chemical and physical weathering in the Min Jiang, a headwater tributary of the Yangtze River

Jianhua Qin [a], Youngsook Huh [b,*], John M. Edmond [c], Gu Du [a], Jing Ran [a]

[a] *Chengdu Institute of Geology and Mineral Resources, Chengdu 610082, Sichuan, P.R.C.*
[b] *School of Earth and Environmental Sciences, Seoul National University, San 56-1 Sillim-dong, Gwanak-gu, Seoul 151-742, Korea*
[c] *Department of Earth, Atmospheric and Planetary Sciences, Massachusetts Institute of Technology, 42 Carleton Street, Cambridge, MA 02139, U.S.A.*

Received 24 December 2004; received in revised form 13 August 2005; accepted 15 September 2005

Abstract

The Min Jiang is a major headwater tributary of the Yangtze (Chang Jiang). Its source is in the undeveloped eastern Tibetan Plateau, but it flows through the heavily populated Sichuan (Four Rivers) Basin on its way to join the Yangtze main channel. The dissolved major element composition was determined in the Tibetan headwaters at the rising stage and at four hydrologic stations in a monthly time series. The Min Jiang is alkaline and has high dissolved load compared to other world rivers. Carbonate weathering dominates, especially in the source region of the Min Jiang main channel, and silicate weathering and evaporite dissolution gain some importance in the Dadu He tributary. The Si/(Na*+K) ratios of the dissolved load and the clay mineralogy of the bed material suggest that silicate weathering in the watershed is superficial, i.e. soluble cations are being preferentially leached. Many major elements show lower concentrations at high summer discharge but there is also additional input, such that the concentration–discharge relationship is not purely a result of dilution. The discharge-weighted total dissolved solid (TDS) flux, based on data from the three upstream monitoring stations, is 10×10^6 tons/year, ~6% of the Yangtze at mouth, and the chemical denudation rate as measured by TDS yield is 115 tons/km^2/year for the Min Jiang, higher than the average Yangtze basin (85 tons/km^2/year). The common extrapolation using annual average discharge and spot sampling of dissolved and suspended material during rising or falling stage can reasonably estimate chemical fluxes to ±20% but seriously underestimate the physical flux. Sampling the peak flash flow is critical for the suspended particulate material. Concentrations of SO_4, Cl and Ca are significantly elevated as the river debouches onto the populated Sichuan Basin.

Keywords: Major element geochemistry; Hydrologic station; Tibetan Plateau; Time series; Changjiang; Monitoring

1. Introduction

Chemical weathering is an important sink of atmospheric CO_2 over geologic timescales (>10^6 years). It supplies nutrients and trace elements from the lithosphere to the biosphere and controls the delivery of material from continents to the oceans. The study of large rivers allows one to explore at regional scales chemical weathering rates and the many parameters that influence them (West et al. (2005) and references therein). The Yangtze River (Chang Jiang) is the fourth largest in the world and the largest in Asia in terms of water discharge (900 km^3/year). Its headwaters drain the Tibetan Plateau, the most prominent feature on Earth today, and the rates of physical and chemical

* Corresponding author. Tel.: +82 2 880 9167; fax: +82 2 871 3269.
E-mail address: yhuh@snu.ac.kr (Y. Huh).

0009-2541/$ - see front matter © 2005 Elsevier B.V. All rights reserved.
doi:10.1016/j.chemgeo.2005.09.011

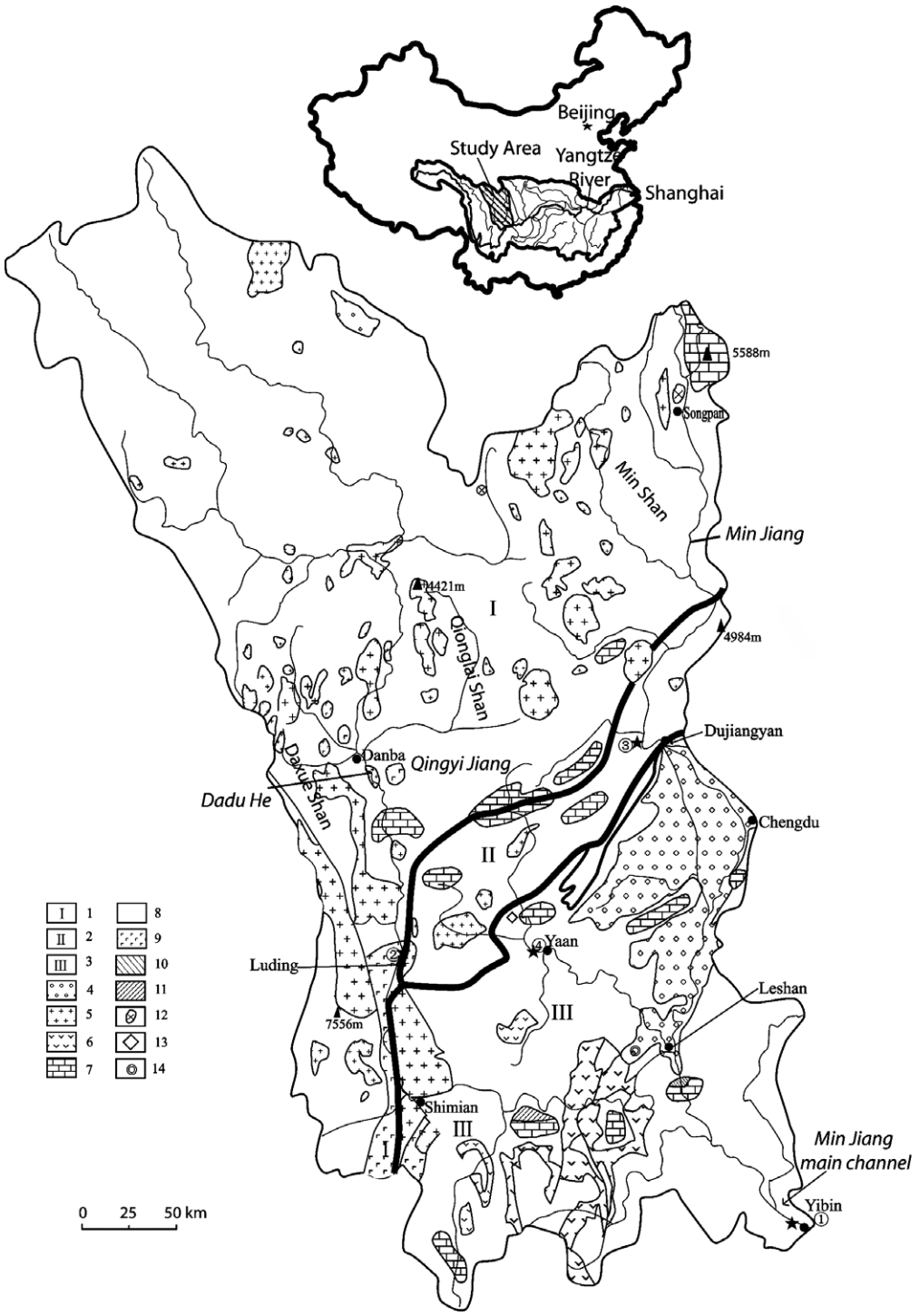

Fig. 1. The Min Jiang drainage basin divided by the thick lines into three geotectonic regions and showing simplified geology (Bureau of Geology and Mineral Resources of Sichuan Province, 1991; Pan et al., 1997, 2002; Research Center of Tibet Plateau Geology, 2002). Keys: 1. Bayan-Har Fold Belt; 2. Longmenshan Fold Belt; 3. Sichuan Basin; 4. Quaternary fluvial deposits; 5. Granites; 6. Volcanic rocks; 7. Carbonates; 8. Terrigenous sediments including low-grade metamorphic rocks; 9. High-grade metamorphic rocks; 10. Gypsum mine; 11. Halite mine; 12. Gold mine; 13. Pyrite mine; 14. Cement factory. ●City, ▲Peak, ★Monitoring stations: ① Gaochang on Min Jiang; ② Luding on Dadu He; ③ Xuankou on Upper Min Jiang; ④ Duoyinping on Qingyi Jiang.

weathering there is of interest for constructing geomorphologic models as well as models of long-term climate evolution (Clark et al., 2004; Raymo and Ruddiman, 1992). However, earlier research on the major element geochemistry of the Yangtze (Hu et al., 1982) and more recent studies (Chen et al., 2002; Zhang et al., 1990) leave a gap in our understanding of the upper reaches in and around the Tibetan Plateau and of the seasonal variations.

The Min Jiang ("Jiang" is "river" in Mandarin) originates in the eastern margin of the Tibetan Plateau, relatively unaffected by human activities, and flows through the industrialized, agricultural, and heavily populated Sichuan Basin to finally join the Yangtze

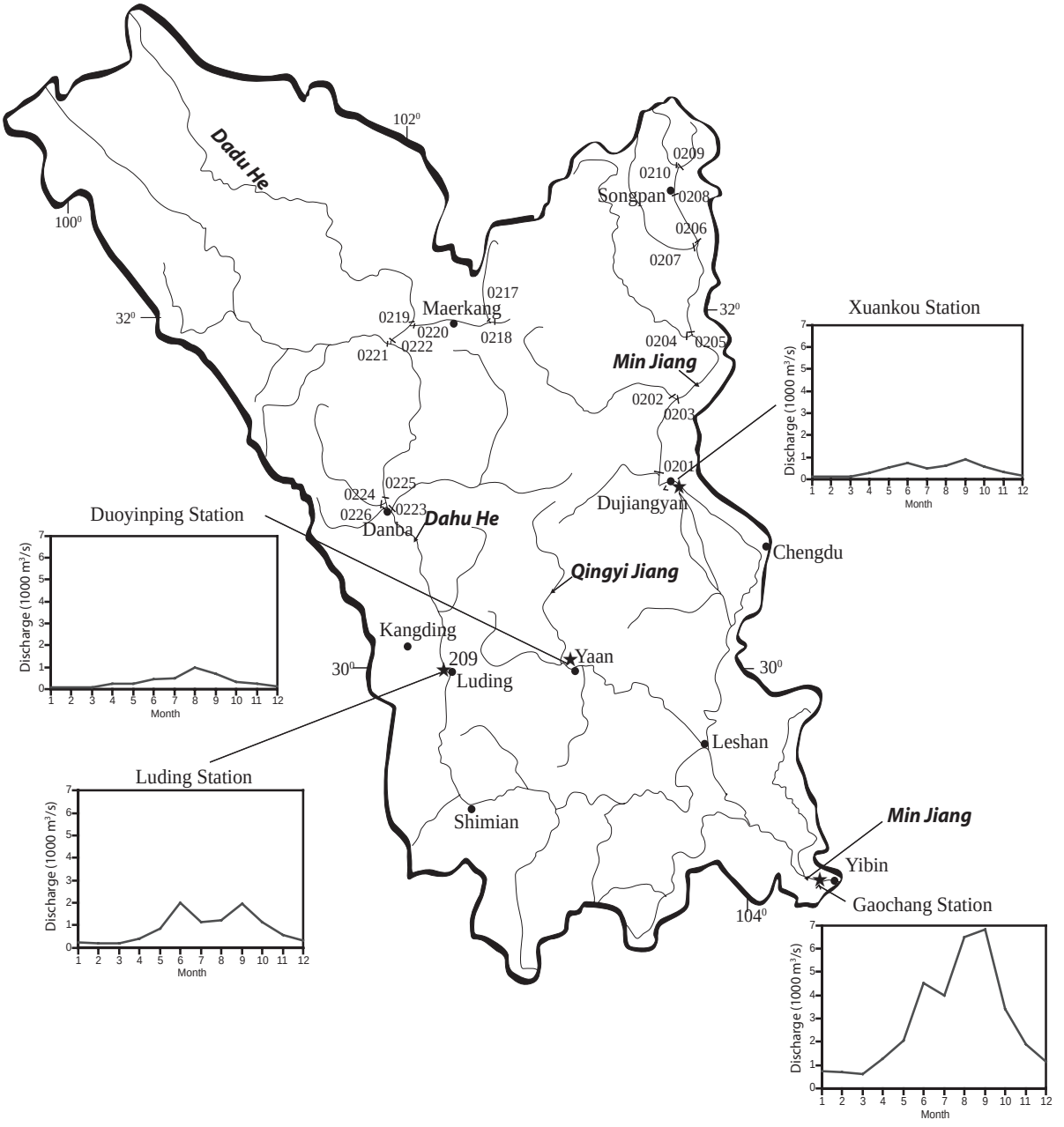

Fig. 2. Location of the headwater and station samples and hydrographs at the four monitoring stations. ●City; ＼0217: Sample location and sample number; ★ Monitoring stations.

main channel at Yibin (Fig. 1). We present analytical results from a summer expedition to the Upper Min Jiang and from a monthly time series study at four hydrologic stations (Fig. 2). We established, based on the contrast in population density, three stations on the eastern Tibetan Plateau to serve as the "natural" baseline and one in the Sichuan Basin to assess the anthropogenic impact. The former three stations are on the Dadu He and Qingyi Jiang tributaries and on the Upper Min Jiang main channel (Luding, Duoyinping, and Xuankou stations, respectively), and the latter one station is just above the confluence with the Yangtze main channel (Gaochang station) (Fig. 2). These four locations coincide with existing hydrologic stations from which we could obtain discharge data for our sampling period. We (1) examine the major element composition of the dissolved load and the clay mineralogy of the bedload to diagnose the main lithologic type undergoing weathering and the intensity of weathering in the drainage basin, (2) quantify the contribution of rain, evaporite, carbonate, and silicate to the dissolved load, and (3) calculate the chemical and physical weathering rates using discharge data from hydrologic stations, appraise the relationship between elemental concentrations, chemical and mechanical weathering fluxes, and water discharge, and evaluate the uncertainty associated with the flux estimates. Using data from the Upper Min Jiang and its tributaries as the baseline, we discuss qualitatively the anthropogenic impact on the major dissolved elements in the lower Min Jiang as represented by the Gaochang station samples. As anthropogenic impact in China is increasing, this offers an assessment of current natural baseline in fluvial transport of elements.

2. Natural setting

2.1. Topography and geology

The Min Jiang is 793 km long and has two major tributaries, Dadu He ("He" is also "river" in Mandarin) and Qingyi Jiang, which join the main channel at Leshan, below which the river is navigable (Fig. 1). Topographically, the source area of the Upper Min Jiang consists of mountains with peaks above 5500 m, while that of the Dadu He tributary is the Plateau at ~4900 m elevation with undulating hills. The river flows to the south and southeast across orogenic belts cutting gorges more than 1 to 3 km deep (Burchfiel et al., 1995). The elevation change from the Plateau to the Sichuan Basin is abrupt, marked by three north–south running mountains, the Min, Qionglai, and Daxue (Fig. 1). The elevation gain is ~50 m/km in the fronts of the Qionglai and Daxue and ~100 m/km in the Min region (Burchfiel et al., 1995). The Min Jiang above Dujiangyan has steeper relief with a water velocity of up to 6–7 m/s (Bureau of Geology and Mineral Resources of Sichuan Province, 1991). The Sichuan Basin is a fluvial plain with an average elevation of ~500 m.

Within the Min Jiang drainage basin, the eastern Tibetan Plateau is composed of two different geotectonic terrains, the Bayan-Har and Longmenshan fold belts (Bureau of Geology and Mineral Resources of Sichuan Province, 1991) (Fig. 1). The Bayan-Har Fold Belt (Region I in Fig. 1) is a syn-collisional marginal foreland made up mainly of sandstone, shale and slate sparsely intercalated with carbonate and volcanic rocks and of minor continental sandstone and mudstone intercalated with coal seams. Isolated platform carbonates are exposed in the source area of the Min Jiang and Qingyi Jiang and in the mid-reaches of the Dadu He (Fig. 1). Minor gypsum appears in northern Luding (Commission on the Annals of Sichuan Province, 1998). Gneiss, schist, granite, carbonaceous slate and phyllite containing pyrite, and minor basic-ultrabasic rocks can also be seen. In the Cenozoic post-collisional Longmenshan Fold Belt (Region II in Fig. 1), a series of tectonic nappe composed of Paleozoic and Precambrian rocks occur. The lithology is meta-igneous and metasedimentary with carbonaceous slate and phyllite intercalated with marble, carbonate intercalated with clastic rocks and minor carbonaceous shale, and coal-bearing sandstone and mudstone. There are also scattered outcrops of granitic intrusive rocks.

The Sichuan Basin, on the other hand, is a relatively undeformed part of the Yangtze Platform (Burchfiel et al., 1995). The area east of Shimian and south of Yaan is covered by carbonate intercalated with gypsum and halite, sandstone and shale (some coal-bearing), and granite and prominent Permian basalt (the Emeishan basalt) (Bureau of Geology and Mineral Resources of Sichuan Province, 1991; Pan et al., 1997). Gneiss, schist, metasedimentary sandstone and slate, meta-igneous rocks with volcaniclastics can also be seen. Fluvial deposits and reddish sandstone and mudstone cover the rest of the Sichuan Basin within the Min Jiang drainage.

2.2. Climate and soil

The climate is subtropical with the exception of isolated sub-frigid pockets in the Upper Dadu He. The January average temperature in Chengdu is 5.5

°C and the July average 25.6 °C (Map Publishing House of China, 1998). Around Maerkang on the eastern Tibetan Plateau (Fig. 2), winter temperatures are below 0.5 °C and summer temperatures 15 to 17 °C, with annual average below 10 °C (Chinese Academy of Sciences Comprehensive Research Team, 1985). The mean annual precipitation is 1200 to 1500 mm in the Sichuan basin and 500 to 800 mm on the eastern Tibetan Plateau. It is highly seasonal with the rainy period (June to September) accounting for about half of the total annual precipitation (Bureau of Geology and Mineral Resources of Sichuan Province, 1991). Water discharge is likewise highly seasonal (Fig. 2). The hydrographs have two peaks—one from snow melt and one from rainfall (Chinese Academy of Sciences Comprehensive Research Team, 1985) (Fig. 2).

The soil color changes progressively from dark brown on the Tibetan Plateau to yellow near the Sichuan Basin (National Soil Survey Office, 1998). At very high elevations the soils are frozen or form bogs, and in the Basin itself, paddy soil is dominant. The clay minerals in the soils of the eastern Tibetan Plateau are dominantly illite (hydromica), vermiculite, and smectite, with minor kaolinite and chlorite. In contrast, kaolinite, gibbsite and vermiculite dominate in the Sichuan Basin, suggesting higher weathering intensity.

Human activities—industrial/communal effluent and agriculture—can complicate the link between river geochemistry and weathering. The population density on the eastern Tibetan Plateau is 1~25 persons/km^2 but is >100 persons/km^2 in most parts of the Sichuan Basin, reaching >800 in big cities (Map Publishing House of China, 1994). The population of Chengdu is more than 10 million and Leshan more than 3 million. Based on this, we consider all our samples as representing natural weathering except those at Gaochang station in the Sichuan Basin. The Sichuan Basin is a large center of rice-farming, and river courses are channeled for irrigation purposes. Since the mid 1970s the Sichuan Basin area has undergone rapid development. Locally, industries (e.g. cement factories) and mining activities can pose water quality issues (Commission on the Annals of Sichuan Province, 1998) (Fig. 1)—for example, gold mines use NaCN and $CaCO_3$ for refining.

3. Method

The spatial variability in the headwaters of the Min Jiang system was assessed by a sampling expedition to the eastern Tibetan Plateau in May of 2002 (Fig. 2). Samples were collected for dissolved major elements and suspended and bed material. In order to understand the temporal variability, we collected water and suspended sediment samples at four monitoring stations every month throughout year 2001. Duoyinping station is an exception, where samples were collected quarterly with an extra sample during the rainy season of August.

Temperature and pH were measured in the field (Tables 1, 2). Water samples were filtered through 0.45 μm Millipore cellulose nitrate filters within 24 h of collection, and aliquots for Si analysis were acidified with AR grade 1:1 HCl. The major anions (Cl, alkalinity, SO_4), Si, and Sr in the dissolved load were measured at the Sichuan Bureau of Geology and Mineral Resources, and the major cations (K, Na, Ca, Mg) at the Chengdu Institute of Geology and Mineral Resources. The Centers for Rock and Mineral Analysis at these institutions are nationally certified labs. Potassium (K) and Na were determined by flame emission spectrophotometry and Ca and Mg by flame atomic absorption spectrophotometry. Silica was analyzed by colorimetry using silicon–molybdenum blue complex, Cl by silver nitrate volumetric analysis, SO_4 by barium sulfate ($BaSO_4$) turbidimetry, and alkalinity by phenolphthalein and methyl orange end point titration with HCl. Strontium concentration was determined by ICP-OES. Analytical precision is better than 3% for each element. The standard solution and material were all in accordance with the state standards in China, e.g. GBW(E)080166 for the determination of K, Na, Ca and Mg; GBW(E)080167 for SO_4 and Cl; GBW(E)080290 and GBW(E)08091 for C; and GBW(E)080234 for Sr.

The material left on the filters after filtration was air-dried and weighed to obtain the suspended particulate material (SPM) content. The bed material was wet-sieved, and the <200 μm suspension was stirred and allowed to settle. The thin layer of suspended material was filtered, dried, and analyzed for clay mineral composition by X-ray diffraction at the Central Lab of the Southwestern University of Science and Technology in China.

4. Results and discussion

The chemical data are reported for one-time sampling of the Min Jiang main channel and the Dadu He tributary systems (Table 1) and for the time-series samples at four monitoring stations (Table 2). The former will be referred to as “headwater” and the latter as “station” samples.

Table 1
Dissolved major element composition of the Min Jiang headwaters

River name[a]	Sample	Date (mm/dd/yy)	T °C	pH	K μM	Na μM	Ca μM	Mg μM	Cl μM	SO_4[b] μM	HCO_3 μM	Si μM	Sr μM	TDS mg/L	TZ^+ μEq	NICB %
Dadu He system																
Shomo He ab. Shomo	CJ0217	05/20/06	9.4	8.35	7.0	62.9	1040	270	16	90	1430	68	1.7	149	2690	40
LB stream ab. Shomo	CJ0218	05/20/06	7.5	8.49	5.3	46.8	691	267	7	70	1560	106	3.1	142	1968	13
Maer Qu	CJ0219	05/21/06	13.1	8.55	9.1	91.6	695	267	20	30	1690	77	2.3	146	2025	13
Shomo He	CJ0220	05/21/06	14.1	8.56	6.6	62.0	600	338	15	20	1690	83	2.2	143	1944	10
Dadu He bl. Beiwan	CJ0222	05/21/06	13.9	8.66	9.1	86.2	622	285	16	190	1690	53	2.3	158	1910	−9
Duke He	CJ0221	05/21/06	19.3	8.86	13.4	113	818	487	16	270	2440	87	2.0	226	2736	−9
LB trib. bl. Zhonglu	CJ0223	05/22/06	14.6	8.65	13.6	44.5	680	378	13	140	1750	49	1.5	160	2175	6
Geshiza He	CJ0224	05/22/06	14.0	8.50	15.7	34.5	506	140	7	100	1170	41	0.8	108	1341	−3
Dadu He ab. Danba	CJ0225	05/22/06	16.6	8.68	12.7	106	651	279	18	90	1850	58	1.8	160	1979	−4
Trib. Ab. Danba	CJ0226	05/22/06	14.7	8.70	13.2	71.0	733	565	7	90	2210	58	1.7	190	2680	11
Dadu He ab. Luding	CJ209	06/02/04	16.6	8.11	12.1	51.3	615	264	15	140	1560	49	1.5	143	1821	−2
Min Jiang system																
Source of Min Jiang	CJ0210	05/18/06	6.8	8.55	12.3	97.5	945	316	22	30	2480	83	2.3	206	2633	3
LB trib. ab. Chuanzhushi	CJ0209	05/18/06	7.3	8.22	10.8	44.5	1500	533	22	20	4020	77	4.0	323	4122	1
Min Jiang ab. Songpan	CJ0208	05/18/06	8.7	8.57	12.1	80.7	1380	493	27	140	3560	87	2.9	303	3839	−1
Min Jiang ab. Zhengjiangguan	CJ0206	05/17/06	14.8	8.84	13.0	82.3	1140	695	28	140	3470	58	3.3	291	3765	0
Riwu Qu	CJ0207	05/17/06	15.1	8.80	10.8	99.1	829	599	23	190	2800	91	2.5	243	2966	−8
Min Jiang bl. Shidaguan	CJ0205	05/17/06	16.1	8.83	14.4	88.7	1080	723	28	140	3210	96	3.0	276	3708	5
Heishiu He	CJ0204	05/17/06	15.0	8.64	10.6	58.7	593	273	23	90	1590	87	1.7	142	1801	0
Min Jiang ab. Yanmen	CJ0203	05/17/06	16.1	8.40	12.5	71.0	807	462	26	90	2240	77	2.3	194	2622	7
Zagulao	CJ0202	05/17/06	14.6	8.36	16.1	53.9	865	313	21	310	1560	77	1.9	173	2426	9
Min Jiang ab. Yinxiou	CJ0201	05/17/06	16.8	8.57	14.0	63.6	776	403	31	170	2050	49	2.1	186	2435	1

[a] ab.=above, LB=left bank, bl.=below, trib.=tributary.
[b] Analytical uncertainty is ±10%.

Table 2
Dissolved major element composition of the Min Jiang monitoring station samples

Sample	Date (mm/dd/yy)	T °C	pH	K μM	Na μM	Ca μM	Mg μM	Cl μM	SO_4[a] μM	HCO_3 μM	Si μM	Sr μM	TDS mg/L	TZ^+ μEq	NICB %
Luding station (Elevation 1780 m) on Dadu He															
LD0101	01/14/05	10.4	8.44	20.4	137	1120	496	39	330	2570	119	4.3	255	3390	4
LD0102	02/19/05	17.6	8.46	22.1	143	1010	484	36	340	2540	119	3.1	250	3152	−3
LD0103	03/17/05	18.9	8.66	17.6	150	1140	493	43	270	2540	124	3.2	249	3434	9
LD0104	04/22/05	18.3	8.46	16.4	104	1580	406	35	290	2020	127	2.3	234	4093	36
LD0105	05/21/05	28.3	8.37	13.0	77.5	751	332	18	150	1950	111	2.0	179	2256	−1
LD0106	06/17/05	28.6	8.36	13.0	60.0	809	279	8	210	1560	111	1.6	162	2249	12
LD0107	07/15/05	30.3	8.46	13.8	68.7	785	332	10	220	1920	124	1.9	186	2315	−2
LD0108	08/19/05	23.1	8.34	13.0	65.2	769	319	11	210	1670	111	1.9	168	2255	7
LD0109	09/21/05	17.5	8.62	14.4	68.4	865	354	7	220	1930	176	2.0	193	2520	6
LD0110	10/18/05	13.9	8.45	14.9	80.7	823	372	13	150	2000	119	2.1	186	2485	7
LD0111	11/16/05	10.4	8.57	14.7	94.2	912	409	16	150	2200	124	2.4	204	2751	9
LD0112	12/21/05	5.8	8.36	17.8	127	954	468	25	150	2340	139	2.8	217	2989	11
Xuankou station (Elevation 834 m) on Min Jiang															
XK0101	01/15/05	5.5	8.41	18.5	102	985	413	29	310	2340	93	3.0	229	2916	−3
XK0102	02/16/05	8.6	8.53	18.5	108	959	524	34	270	2440	124	3.1	235	3092	3
XK0103	03/14/05	12.6	8.57	24.0	118	1670	658	43	290	2510	86	3.1	272	4797	35
XK0104	04/15/05	13.4	8.56	20.6	90.0	1570	487	29	170	2080	86	2.7	225	4224	42
XK0105	05/14/05	15.7	8.56	17.8	61.0	878	319	17	50	1820	71	2.0	164	2474	22
XK0106	06/16/05	17.2	8.38	16.4	51.0	1540	316	9	120	1660	78	1.8	187	3780	50
XK0107	07/19/05	19.2	8.58	17.2	61.3	2650	409	13	170	1740	78	2.2	244	6197	66
XK0108	08/23/05	17.2	8.52	16.8	47.8	987	270	9	150	1690	71	1.8	168	2579	23
XK0109	09/18/05	17.7	8.53	16.8	52.3	1150	276	8	210	1630	78	1.9	178	2921	30
XK0110	10/16/05	14.9	8.49	17.4	60.0	1970	397	14	190	1920	86	2.2	230	4812	52
XK0111	11/14/05	11.5	8.51	15.5	68.7	905	369	19	270	2060	96	2.4	203	2632	1
XK0112	12/14/05	6.6	8.38	16.4	87.8	945	444	28	240	2110	89	2.7	207	2881	9
Duoyinping station (Elevation 671 m) on Qingyi Jiang															
YA0103	03/16/05	19.4	8.14	11.0	82.3	889	397	31	310	1820	74	2.7	192	2666	7
YA0106	06/17/05	28.4	7.96	18.5	93.6	936	214	30	260	1560	68	2.0	169	2412	13
YA0108	08/25/05	29.1	8.30	11.0	50.3	963	313	22	220	1630	86	1.8	173	2614	20
YA0109	09/22/05	17.7	8.62	10.8	49.1	914	313	16	170	1790	86	1.8	175	2514	15
YA0112	12/22/05	6.4	8.19	11.3	87.1	979	422	33	330	1920	81	2.6	205	2899	10
Gaochang station (Elevation 303 m) on Min Jiang															
GC0101	01/20/05	9.6	8.14	26.5	431	1200	484	260	600	2340	131	3.5	286	3826	1
GC0102	02/18/05	11.7	8.22	24.6	427	1160	475	184	450	2460	127	3.9	273	3720	5
GC0103	03/18/05	16.3	8.11	27.6	399	1530	527	228	480	2460	109	3.7	292	4541	20
GC0104	04/22/05	19.1	8.15	24.2	269	1010	431	151	310	2200	109	2.9	231	3175	6
GC0105	05/19/05	19.4	8.28	24.8	145	941	366	100	270	1950	124	2.4	205	2783	7
GC0106	06/21/05	21.3	8.12	21.7	111	860	301	75	270	1750	124	2.1	186	2455	4
GC0107	07/22/05	25.9	8.36	21.4	136	2300	431	79	140	2020	124	2.5	251	5619	58
GC0108	08/22/05	21.7	8.26	29.3	119	1030	257	129	270	1800	109	2.2	196	2723	9
GC0109	09/20/05	22.4	8.36	24.0	138	1050	347	92	260	2050	124	2.4	213	2957	10
GC0110	10/21/05	17.4	8.31	20.4	160	1090	406	103	330	2180	134	2.7	232	3173	7
GC0111	11/21/05	13.7	8.16	21.9	216	1420	453	138	380	2240	113	3.0	256	3983	21
GC0112	12/19/05	9.5	8.08	24.0	255	1220	481	157	380	2340	108	3.2	256	3680	11

[a] Analytical uncertainty is ± 10%.

4.1. Dissolved major elements

The surface water temperatures of the headwater samples vary from 7 to 19 °C with the lower values found in mountainous source regions (Table 1, Fig. 2). The station samples show seasonal variation, which is largest at Luding and Duoyinping stations (6 °C in winter and 30 °C in summer) (Table 2). The samples are all very alkaline with pH values from 8.0 to 8.9.

The total cationic charge ($TZ^+ = Na^+ + K^+ + 2Mg^{2+} + 2Ca^{2+}$) as a measure of total dissolved content range from 1300 to 4100 μEq (10^{-6} charge equivalent units

per liter) in the headwater samples, higher than the estimated world average of 1125 μEq (Meybeck, 2003). The low end is for a small Dadu He tributary (CJ0224) draining igneous rocks and terrigenous sediments (Figs. 1, 2). The high end is for sample CJ0209 draining the carbonates north of Songpan, near the famous Huanglong tufa deposits (Yoshimura et al., 2004), and is diluted downstream along the Min Jiang main channel (CJ0209, CJ0208, CJ0206, CJ0205)(Fig. 1). The TZ^+ values for station samples are variable with time, usually lower during the summer flood period and higher in the winter lean period (Table 2). The total dissolved solid (TDS) is calculated as $Na+K+Ca+Mg+CO_3+Cl+SO_4+SiO_2$. There is a general correlation between TDS and TZ^+, and the range in TDS (108 to 322 mg/L) is defined by the same two samples. All Luding station samples (2200 to 4100 μEq) have higher TZ^+ than the Dadu He sample (CJ209) collected above the station, and all Xuankou station samples (2500 to 6200 μEq) are higher than the Min Jiang sample (CJ0201) above the station. The sharp decrease in TZ^+ between April and May at these two stations presumably result from dilution by snowmelt. The Xuankou samples show seasonally erratic TZ^+ with extreme values in March, July and October. Duoyinping station samples are relatively stable throughout the year (2400 to 2900 μEq). Of the four stations, Gaochang has the highest TZ^+ (2500 to ~5600 μEq) with extreme values in March and July.

In most world rivers, the measured major elements (K, Na, Ca, Mg, Cl, alkalinity, SO_4, and Si) account for most of the dissolved load, and the Normalized Inorganic Charge Balance ($NICB=(TZ^+-TZ^-)/TZ^+$, where $TZ^-=Cl^-+HCO_3^-+2SO_4^{2-}$ in μEq) is used to estimate overall analytical uncertainty (Tables 1 and 2). NICB should ideally be close to zero, unless one or more ions have been overlooked in the analyses. There are large charge imbalances in the samples from the headwaters of the Dadu He (CJ0217) and in some Xuankou and Gaochang station samples, especially for March and July. This is far in excess of the analytical error and suggests the existence of unanalyzed anions. In the Orinoco, the large NICB (up to ~1) was observed in "black" rivers with low TZ^+ (<100 μEq) draining the Guayana Shield, and organic acid anions were presumed to be responsible (Edmond et al., 1995). However, in the Min Jiang, the high NICB occurs in samples with high TZ^+ (>2000 μEq). This imbalance occurs largely due to very high Ca relative to HCO_3. We suspect that pulses of Ca associated with unmeasured anions (e.g. nitrate, phosphate, organic) from anthropogenic sources (e.g. fertilizer, detergent) may be responsible for the high NICB in station samples. If dissolved reactive phosphorus concentrations in June in the Dadu He region (Huh, unpublished data) can be taken as representative, these sub-micromolar values are insufficient to account for the large NICB. The nitrate levels at the three headwater stations are also in the 2–40 μM range (data from the Sichuan Hydrologic Bureau). However, we cannot discount large flash inputs of these nutrients that were missed in spot sampling. In the case of the Dadu He sample (CJ0217), the gold mine upstream or the relatively high organic carbon content of the Triassic slate and siltstone may be responsible.

Both the headwater and station samples define a narrow range on ternary diagrams typical of carbonate dissolution, not only those draining significant outcrops of carbonate but also those draining large swaths of terrigenous sediments (Figs. 1, 3). Among the world rivers draining orogenic zones, the Mackenzie River has a similar major ion composition (predominantly carbonate) as the Min Jiang system. A comparison of the ternary diagrams shows that the silica levels are comparatively low in both systems, though on an absolute scale, the Mackenzie has lower values (many samples below 40 μM) (Millot et al., 2003). Compared to the headwater samples, the station samples have higher Ca and (Na+K). Silica contribution is overall minor, but the station samples have slightly higher Si and a larger range in $Cl+SO_4$. Winter samples (Jan, Feb, Mar) from Gaochang station have high (Na+K), and the well-balanced Na and Cl suggests that halite dissolution is responsible. The high SO_4 can come from pyrite, as is suspected for sample CJ0202 of the Min Jiang system draining Silurian phyllite (Chen, oral communication) and the Duoyinping station with many pyrite mines upstream ($(Cl+SO_4)$ is 20–25% on the ternary diagram) (Fig. 1). Dissolution of evaporites (halite and gypsum) in the Sichuan Basin (see mine locations in Fig. 1) is more likely the case for the Gaochang station samples ($(Cl+SO_4)$ is 20–37% on the ternary diagram) judging from high Na and Cl along with SO_4.

The dominance of carbonate can also be demonstrated in Mg–Ca space based on end member ratios from monolithologic terrains (Gaillardet et al., 1999) (Fig. 4). The samples lie very close to the carbonate end member, with CJ0209, the high TZ^+ sample above Songpan, defining the end member composition itself. July and October samples of the Xuankou station are also close to the carbonate end member, but this may be due to sporadic anthropogenic effect on Ca as mentioned

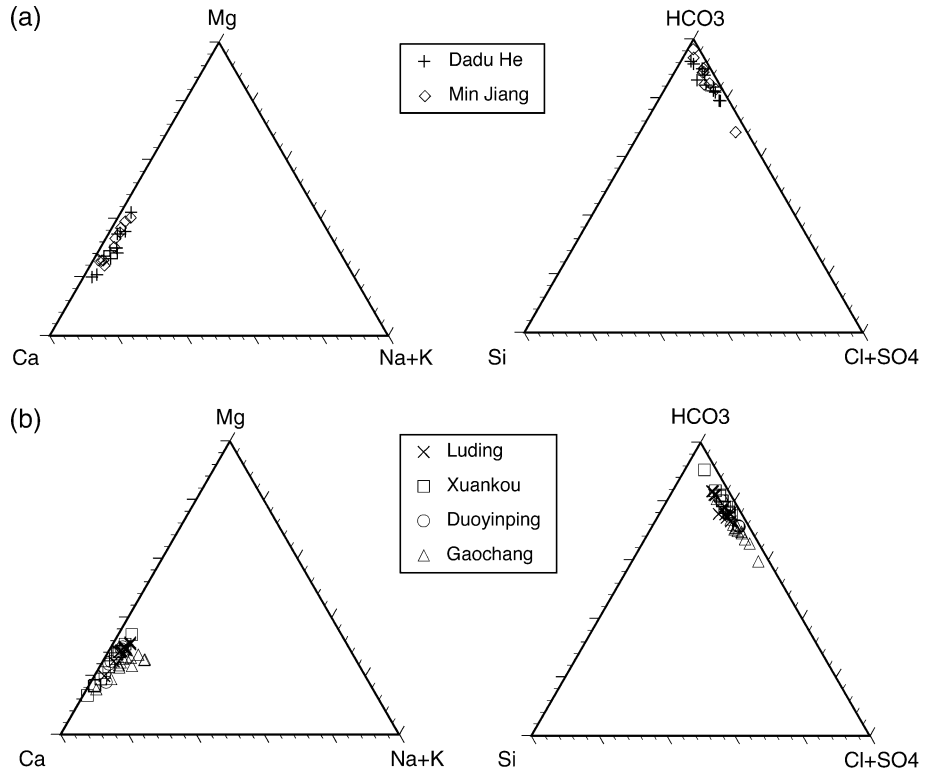

Fig. 3. Ternary diagrams for (a) headwater and (b) monitoring stations indicating dominance of carbonate weathering. The data are in charge equivalent units (μEq) and are not corrected for atmospheric input.

above. The Gaochang station winter samples show mixing with evaporites.

Most Sr concentrations in the river studied here are above 1 μM, greater than the global average of 0.89 μM (Palmer and Edmond, 1989). The Min Jiang headwater samples and Luding and Gaochang station samples (with the exception of April Luding and July Gaochang) show a broad correlation between Sr and Ca. The Sr/Ca molar ratios are higher than expected for carbonates (0.7) but lower than for shales and sandstones (5), and the significant scatter between these two book-end values reflect the diverse lithologies with different parent Sr/Ca ratios at various stages of weathering and also the possible incongruent weathering of trace Sr (Bullen et al., 1997). The July and October samples of the Xuankou station have extremely high Ca relative to Sr, reinforcing the possibility of anthropogenic input.

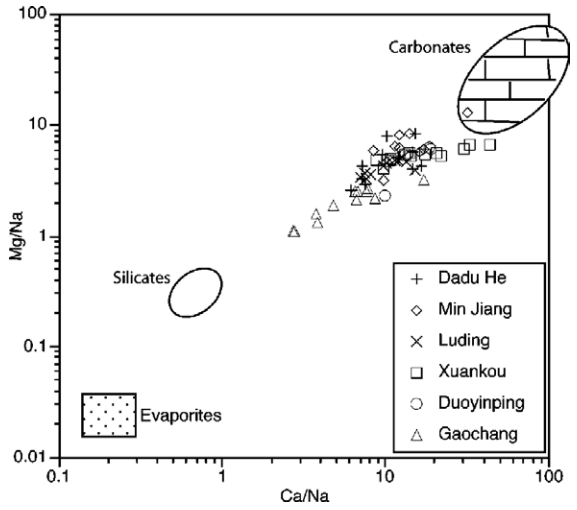

Fig. 4. Molar ratios of Mg/Na and Ca/Na not corrected for atmospheric input. End member compositions for carbonate, silicate and evaporite are slightly modified from Gaillardet et al. (1999).

The calcite saturation index (CSI) is defined as log $(\{Ca^{2+}\}\{CO_3^{2-}\}/K_{calcite},)$, where {} denotes activity. We calculated this with the Geochemist's Workbench® (Bethke, 2002), using water temperatures measured in the field. The samples are all supersaturated as is commonly seen in other carbonate rivers (Huh et al., 1998). The saturation of the Min Jiang increases downstream from the high-carbonate CJ0209 sample, and the Xuankou station samples are the most supersaturated among the station samples.

Perhaps the most direct evidence of silicate weathering is the level of dissolved Si, which varies between

40 and 110 μM in the headwater samples (Table 1). In the station samples the concentrations range from 60 to 170 μM with no obvious seasonality (<30% variability except for two extreme samples) (Table 2). The world average is 145 μM (Meybeck, 2003). The Si/(Na*+K) molar ratio, where Na* indicates correction for halite (Na–Cl), is a measure of the intensity of silicate weathering. As an example, albite weathering to kaolinite generates a ratio of 2, whereas albite to gibbsite yields a ratio of 3. The Si/(Na*+K) ratios in both headwater and station samples fall between 1.7 (representing weathering of average shield to kaolinite) and 1.0 (representing weathering of average shale to kaolinite). If variability in source composition is negligible, this indicates that silicate weathering is superficial. Exceptions are a winter Gaochang sample with extremely low ratio and a summer Gaochang sample with extremely high one. There is a general seasonality, with high ratios in summer and low ratios in winter, which is generally driven by variations in Na rather than Si. Biologic processes—grass and rice stalks taking up Si to build phytoliths and diatoms using Si to build their shells in stagnant waters—which would drive the ratios lower during the spring–summer growing season do not appear to be significant in the watershed.

Supporting evidence for superficial silicate weathering is supplied by analyses of the clay minerals of the bed material. Clay minerals make up 70~90% of <200 μm fraction in the bed load. Table 3 shows that the clay minerals of the bed material are composed mainly of illite plus sericite (55~75%) and minor chlorite and smectite. This reflects the low-grade metamorphic source rocks of the area, and the cation-rich nature of these clay minerals suggests that weathering is still at an incipient stage.

4.2. Sources of solutes in the Min Jiang system

Determining the origin of the solutes in the rivers is a non-trivial task, as is evidenced by the various approaches used to estimate the silicate-derived fraction, an important parameter in calculating long term CO_2 uptake rates by chemical weathering. Methods such as forward modeling using end member Ca/Na or Mg/Na ratios of bedrock (Galy and France-Lanord, 1999; Krishnaswami et al., 1999) or using Sr isotope ratios (Edmond and Huh, 1997), inversion method (Négrel et al., 1993), and using arrays of water compositions to constrain the end member element ratios (Bickle et al., 2005) appear in the literature. In all the above methods, assignment of end member element ratios is critical, and the relative uncertainties in the calculated silicate weathering rates are on the order of 30% (Wu et al., in press). We have used the forward modeling approach to calculate the contributions of rain, evaporite, carbonate and silicate.

In order to examine the lithologic origin of the dissolved load, one first needs to correct for input from the atmosphere. This is frequently done by correcting for marine aerosol assuming all the Cl in the river is from seasalt. Since the Min Jiang basin is relatively far from marine influence, we chose to use literature values for rainwater composition instead. With this approach, weathering of mineral dust by rain water in the atmosphere is included in the "atmosphere" and not in the respective lithologic category. We used (1) data for the Tibetan Plateau for the headwater samples and the three upstream stations (Zhang et al., 2003) and (2) data for the Sichuan Province for the Gaochang station (Environmental Protection Bureau of Sichuan Province, 2002) (Table 4). The SO_4 concentrations are higher and HCO_3 concentrations lower in the rain of the Sichuan Province than on the Tibetan Plateau as expected from the higher population and use of high-S coal. The S aerosol decreases with elevation and shift towards the east from the major centers of sulfur emission, Chongqing and Guiyang southeast of the Min Jiang basin, and we do not expect the effect of atmospheric S deposition to be significant in most of the Min Jiang drainage basin except at the Gaochang station. We took the lowest Cl concentration (7 μM) as being supplied entirely by atmospheric input and subtracted the rain component

Table 3
Relative content of clay minerals in the bed load

River name	Sample number	Chlorite (%)	Illite+sericite (%)	Smectite (%)
Dadu He ab. Luding	CJ209	28	72	–
Heishiu He	CJ0204	40	55	5
LB trib. bl. Zhonglu	CJ0223	22	74	4
Geshiza He	CJ0224	36	57	7
Dadu He ab. Danba	CJ0225	36	57	7
Min Jiang ab. Yinxiou	CJ0201	22	66	12

Table 4
Rainwater composition used for atmospheric input correction

Location	Year	K, μM	Na, μM	Ca, μM	Mg, μM	Cl, μM	SO_4, μM	HCO_3, μM	Reference
Three remote towns in Tibet	1987–1988	9.5	23.2	139.7	5.7	21.2	1.6	199.5	
(Amdo, Dangxiong, Dingri)	1998–2000	10.3	12.1	93.2	10.4	2.9	6.0	137.0	Zhang et al. (2003)
	1987–1988	14.8	89.0	150.3	5.7	21.7	2.5	288.9	
Lhasa	1998–2000	5.1	11.2	197.4	10.9	9.7	5.2	231.7	
Sichuan	2000	40.5	21.4	84	12.3	51	122		EPBSP (2002)
	2001	11.2	16.7	160	12.8	35	142	55.3[a]	

[a] Calculated by charge balance.

from other elements based on the X/Cl ratios of the rain data. The rain correction makes the greatest difference to Na (up to 46%) and K (up to 88%) and is less than ~15% for Ca, Mg and SO_4 and affects headwater and the 3 upstream station samples more than the Gaochang station ones.

We assumed all Cl after atmospheric correction to be from halite and all sulfate from gypsum dissolution and assigned equivalent amounts of Na and Ca to evaporite-origin. It is difficult to distinguish the source of sulfate between gypsum, pyrite, and anthropogenic origins using only the major elements. The above assumption can underestimate carbonate- and silicate-derived Na and Ca accompanying sulfide oxidation, as could be important for CJ0202 and Duoyinping station samples. If we apply the rainwater correction to the Gaochang station samples, the sulfur input from the atmosphere in the form of acid rain is on average only ~7% of that in the river dissolved load. For silicate fraction, we assumed a Ca/Na ratio of 0.7 and Mg/Na ratio of 0.3 and assigned all the Na after evaporite and rain correction to silicate source. Carbonate fraction is calculated as the remainder of the Ca after rain and evaporite correction. The result is that on average carbonate weathering accounts for 70% (range 40–90%) of total cations in the dissolved load, whereas evaporite accounts for 15% (2–40%), and silicate and atmospheric input is minimal at 7% (1–24%) and 6% (1–13%), respectively (Fig. 5).

4.3. Temporal variation in composition

The time series measurements at monitoring stations indicate that K, Na, Mg, Cl, SO_4, HCO_3, and Sr decrease with increasing discharge (Fig. 6). This is best fit to equation,

$$C_i = a \cdot Q^{-b}$$

where C_i is the concentration of element i and Q is the water discharge. Such behavior has been commonly reported, for example by Nkounkou and Probst (1987), and the value for b is usually greater than 1 (Fig. 6). In the case of the Min Jiang, b is significantly lower than 1, requiring an additional source that compensates for the dilution. In weathering-limited (vs. transport-limited) regimes where the transport rate exceeds the ability of weathering processes to generate the material to be transported (Stallard and Edmond, 1983), increase in water discharge leads to dilution. On the other hand, in transport-limited systems more material is available for transport with higher water discharge such that the total flux increases. In the case of Ca, the extreme values obscure any relationship to discharge, and Si does not show significant variation temporally (Fig. 6).

4.4. Flux calculations and uncertainty analysis for spot sampling

The suspended particulate material (SPM) was measured for the station samples (Table 5), but because our samples are not depth-integrated, the SPM values can have large uncertainties. The SPM is mainly delivered by the first high discharge in late spring (June samples

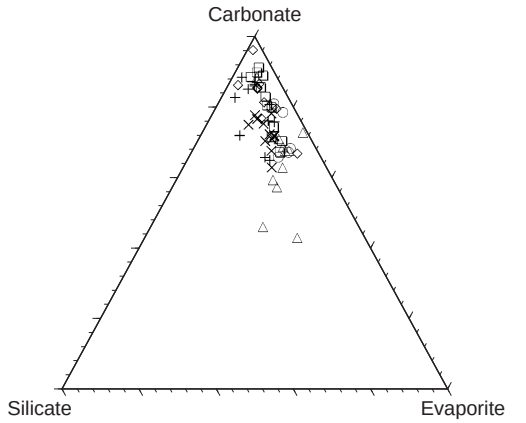

Fig. 5. The fractions of total cations (in molar units) derived from evaporite, carbonate, and silicate, calculated by forward modeling. See Section 4.2. for assumptions used. Legend is same as in Fig. 4.

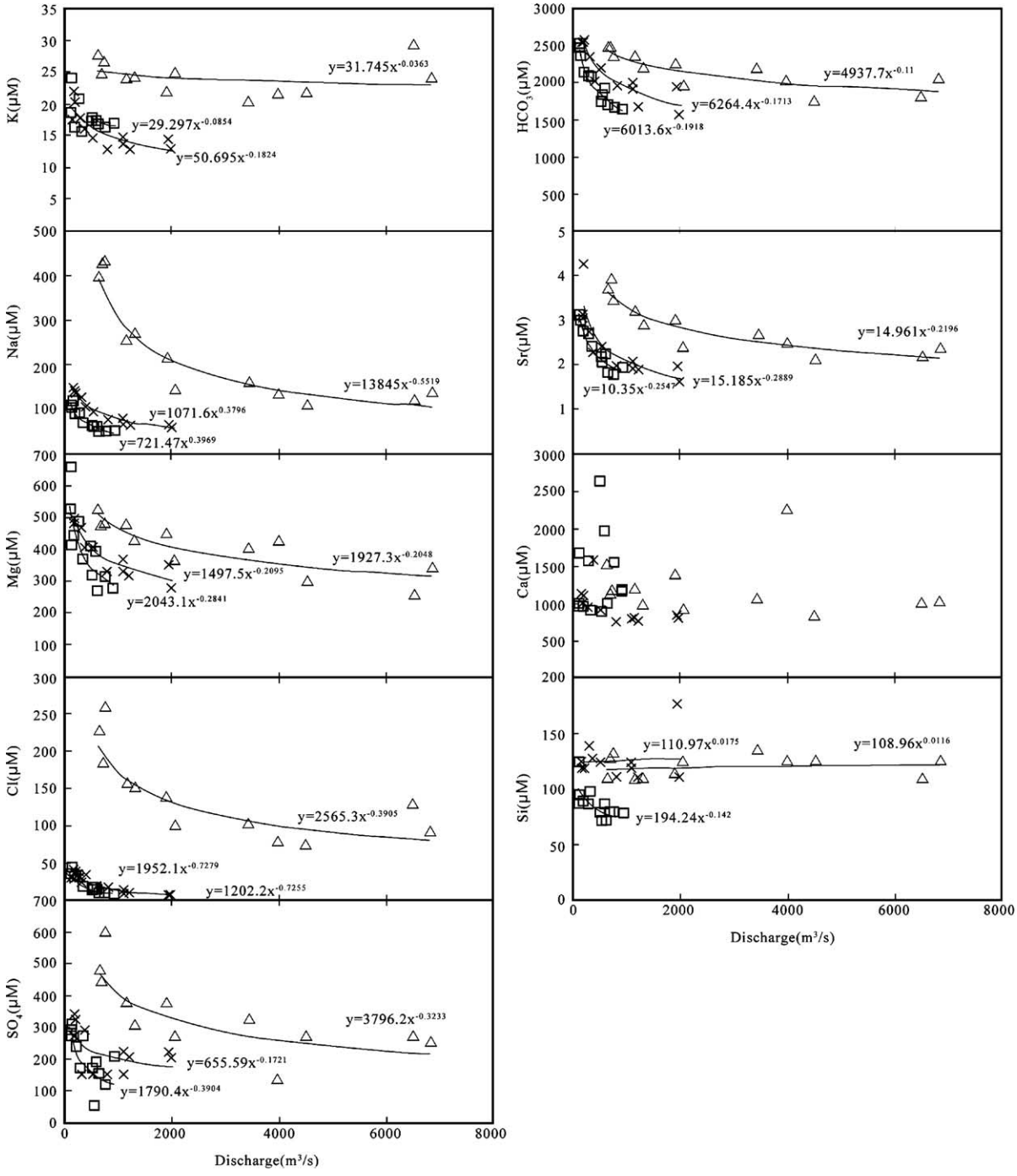

Fig. 6. Relationship between concentration and water discharge for major elements. Concentrations decrease with increasing discharge except for Si and Ca, but the effect is not entirely dilution.

reach 4000 mg/L) and is negligible at other times of the year (tens of mg/L and lower than the TDS). We think this is due to sediment settling en route during low energy periods and to flushing out effect at high-energy flood events. We used the station data to calculate the TDS and SPM fluxes as measures of the chemical and physical weathering rates. We multiplied the TDS and SPM (mg/l) of the monthly sample that we analyzed by the average monthly discharge (m^3/s) measured at near-by hydrologic stations and averaged over 1 year (Table

Table 5
Calculation of fluxes and yields of TDS (total dissolved sediment) and SPM (suspended particulate material)

Sample number	Water discharge[a] m^3/s	Runoff mm/year	TDS mg/l	SPM mg/l	TDS flux 10^6 tons/year	SPM flux 10^6 tons/year	TDS yield t/km^2/year	SPM yield t/km^2/year
Luding station (58,600 km^2) on Dadu He								
LD0101	226	122	255	21	1.82	0.15	31.0	2.6
LD0102	205	110	250	21	1.61	0.14	27.6	2.3
LD0103	197	106	249	13	1.55	0.08	26.4	1.4
LD0104	412	222	234	174	3.04	2.26	51.9	38.6
LD0105	836	450	179	82	4.72	2.16	80.6	36.9
LD0106	2010	1082	162	4224	10.25	267.75	175.0	4569.1
LD0107	1130	608	186	69	6.62	2.46	112.9	42.0
LD0108	1240	667	168	35	6.57	1.37	112.1	23.4
LD0109	1970	1060	193	41	12.00	2.55	204.8	43.5
LD0110	1130	608	186	41	6.64	1.46	113.4	24.9
LD0111	551	297	204	16	3.54	0.28	60.4	4.7
LD0112	329	177	217	7	2.25	0.07	38.4	1.2
Average	853		207	395	5.05	23.39	86.2	399.2
May[b]					4.82	2.21	82.2	37.6
Xuankou station (22,800 km^2) on Min Jiang								
XK0101	118	163	229	30	0.85	0.11	37.4	4.9
XK0102	110	152	235	27	0.82	0.09	35.8	4.1
XK0103	115	159	272	31	0.99	0.11	43.2	4.9
XK0104	277	383	225	47	1.96	0.41	86.2	18.0
XK0105	527	729	164	51	2.72	0.85	119.5	37.2
XK0106	752	1040	187	70	4.44	1.66	194.8	72.8
XK0107	502	694	244	44	3.86	0.70	169.5	30.6
XK0108	624	863	168	182	3.31	3.58	145.2	157.1
XK0109	908	1256	178	42	5.08	1.20	223.0	52.7
XK0110	579	801	230	32	4.19	0.58	184.0	25.6
XK0111	325	450	203	32	2.08	0.33	91.4	14.4
XK0112	184	255	207	19	1.20	0.11	52.7	4.8
Average	418		212	51	2.63	0.81	115.2	35.6
May[b]					2.16	0.67	94.8	29.5
Duoyinping station (8800 km^2) on Qingyi Jiang								
YA0103	100	357	192	23	0.60	0.07	68.5	8.3
YA0106	457	1638	169	111	2.44	1.60	277.1	181.5
YA0108	940	3369	173	109	5.12	3.23	581.5	367.2
YA0109	705	2526	175	106	3.90	2.35	442.7	266.8
YA0112	138	495	205	10	0.89	0.05	101.3	5.1
Average	468		183	72	2.59	1.46	294.2	165.8
June[b]					2.50	1.63	283.7	185.8
Gaochang station (131,300 km^2) on Min Jiang								
GC0101	736	177	289	45	6.70	1.04	51.0	8.0
GC0102	683	164	281	13	6.05	0.28	46.1	2.1
GC0103	627	151	295	6	5.84	0.12	44.5	0.9
GC0104	1290	310	233	19	9.50	0.77	72.3	5.9
GC0105	2040	490	215	37	13.85	2.38	105.5	18.1
GC0106	4500	1081	197	907	27.92	128.71	212.6	980.3
GC0107	3970	954	258	35	32.28	4.38	245.9	33.4
GC0108	6500	1561	199	339	40.73	69.49	310.2	529.2
GC0109	6840	1643	227	165	48.86	35.59	372.1	271.1
GC0110	3430	824	254	35	27.43	3.79	208.9	28.8
GC0111	1890	454	272	18	16.20	1.07	123.4	8.2
GC0112	1140	274	270	9	9.70	0.32	73.9	2.5
Average	2804		249	136	20.42	20.66	155.5	157.4
May[b]					19.04	3.27	145.0	24.9

[a] Mean monthly discharge obtained from hydrologic stations.
[b] Calculated using only the May data for TDS and SPM and annual average discharge.

5). The flux divided by the drainage area is the yield (tons/km^2/year).

The TDS yield is greatest for the Duoyinping station and lowest for the Gaochang station. Among the various factors that affect TDS yield, variation in water discharge appears to be the most important, generating a good correlation between TDS yield and discharge. If we take as our minimum estimate of the natural chemical weathering rates the average TDS yield of the upper Min Jiang (the three upstream stations 114 t/km^2/year), it is higher than the 85 t/km^2/year of the Yangtze (at Wuhan) (Hu et al., 1982). The TDS yield of both Dadu He (at Luding) and Min Jiang (at Xuankou) draining the Tibetan Plateau at mid-latitudes (~30° N) is similar at the order of magnitude scale as the Mackenzie ($0.66–0.85\times10^6$ mol/km^2/year) draining the Rocky Mountains in the subarctic (Millot et al., 2003).

For the SPM, the Luding station at Dadu He yields more than 20 times the SPM compared to the Xuankou on Min Jiang. This is driven especially by the June sample at Luding when discharge reached maximum and SPM was extremely high. The SPM yield is higher in upstream stations Luding and Duoyinping than in Gaochang station and indicates that the suspended material undergoes storage and removal en route. The SPM and TDS yields correlate on logarithmic scale (Fig. 7). SPM and TDS contents in themselves do not have significant correlation and the apparent coupling between physical and chemical weathering rates is because the variation in discharge is larger than the variation in SPM or TDS.

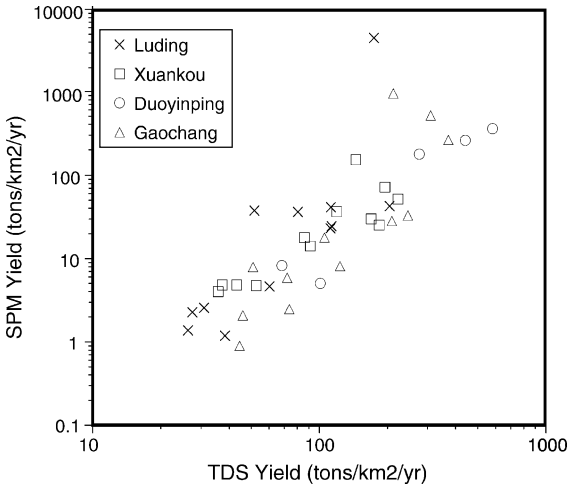

Fig. 7. The relationship between chemical weathering rate (total dissolved sediment yield) and physical weathering rate (suspended particulate material yield).

Table 6
Relative change (%) in the dissolved major element concentrations between upstream stations (Luding, Xuankou, and Duoyinping) and Gaochang station at mouth

Month	K	Na	Ca	Mg	Cl	SO_4	HCO_3	Si
1	35	245	12	3	632	88	−6	19
2	18	226	17	−5	423	40	−2	5
3	55	220	25	2	472	67	4	7
4	34	173	−36	−2	364	27	8	−2
5	67	103	18	12	472	139	3	30
6	49	77	−14	8	575	42	11	27
7	44	104	69	21	640	−34	8	12
8	87	68	18	−6	674	29	10	24
9	98	160	14	9	586	39	14	20
10	30	118	−10	7	680	97	11	25
11	46	154	57	15	700	90	5	0
12	50	137	27	6	469	76	7	−4
Average	51	149	28	9	557	58	8	19

Positive values indicate increase downstream.

Studies of large rivers have been limited logistically, and hence the flux estimates are based on one-time sampling of the dissolved load, usually during rising or falling stages, and annual average discharge modeled with data from a few hydrologic stations. We evaluate the validity of such a method against our monthly monitoring data. Under the hypothetical case of sampling at those four stations in May (the time of our headwater sample collection), we compared the flux estimates between time-series and one-time sampling. In the case of the TDS yield, such one-time sampling, if conducted at rising or falling stage, agrees with time-series sampling estimate (5% for Luding, 19% for Xuankou, 4% for Duoyinping, and 7% for Gaochang) (Table 5). One-time sampling during peak flow months gives the best agreement with time-series estimates (<±10%) and worst if using lean flow periods (up to 37%). Hence, in the absence of time-series measurements of the chemical concentrations and discharge, using TDS data of the one time sample at rising or falling stage and mean annual discharge would yield correct flux estimates within ±20%. Further, if sampling is done during peak discharge, the uncertainty will be below ±15%. Time series sampling becomes a serious issue for SPM flux estimates. One-time sampling in May, for example, can drastically underestimate (~20 vs. ~3) the SPM fluxes. The SPM is delivered in short flash floods, and thus it is critical that the extreme events are sampled. In the case of the Min Jiang, sampling in June, the first peak flow in the year, gives the closest approximation to the annual average physical weathering rate.

4.5. Upstream monitoring stations versus Gaochang station

We assume that anthropogenic impact is minimal above the three upstream monitoring stations and take their discharge-weighted composition as the natural baseline (C_b).

$$C_b = \frac{\sum_{j=1}^{3} C_j \cdot Q_j}{\sum_{j=1}^{3} Q_j}$$

where C_j's are concentrations of an element for the three upstream stations (Luding, Xuankou, and Duoyinping), and Q_j's are the monthly discharge at those stations. Then, we calculate the difference between the downstream Gaochang station and this baseline and attempt to estimate how much of this difference is due to human activity as opposed to natural lithologic variation in the drainage basin.

The concentrations of some ions (Cl, Na, SO_4, K, and Ca) at the Gaochang station show an obvious increase of >20% (Table 6). Lithologic variation, especially increase in volcanic rocks, limestones, halite, and gypsum downstream (Fig. 1), would cause these concentration increases at Gaochang station as can anthropogenic effect. Records from 1976 to 2001, though

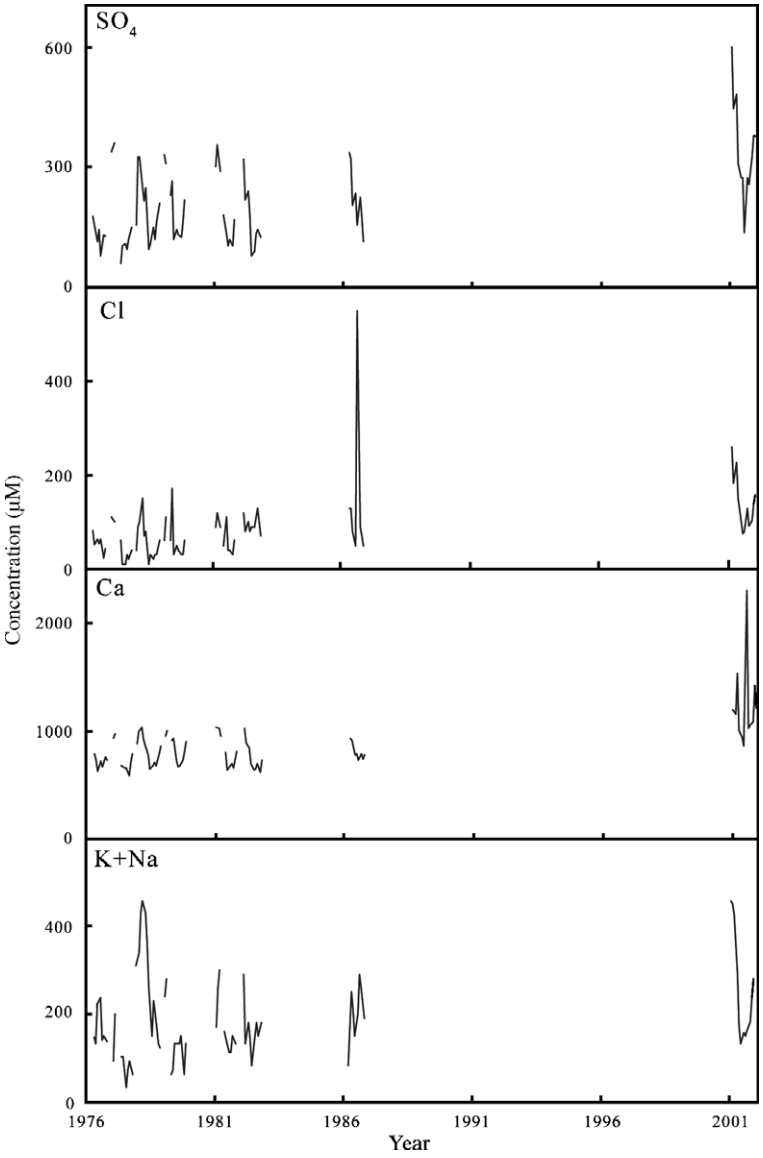

Fig. 8. The time series trend of the concentrations of the major elements during 1976 to 1995 (data from Sichuan Hydrologic Bureau) and our own data for 2001.

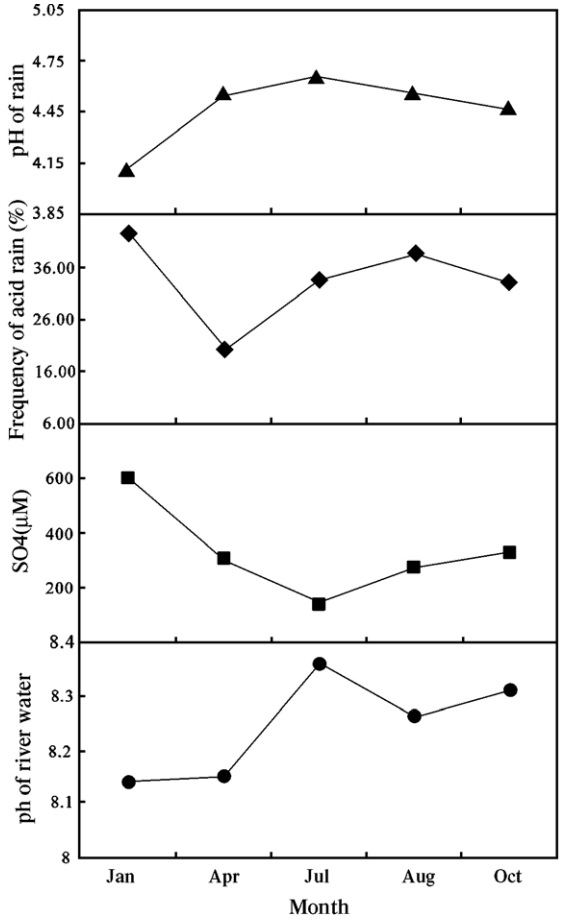

Fig. 9. The covarying relationship between SO_4 and pH of the Min Jiang at Gaochang station and the acidity and frequency of the acid rain in year 2001 in the Sichuan Province.

incomplete, of the concentrations of the above elements show gradual increases in Cl, SO_4 and Ca, in contrast to the random variation for Na and K (Sichuan Head Hydrologic Station, 1984) (Fig. 8). A more complete record from 1962 to 1990 of SO_4 at Gaochang station allowed Chen et al. (2002) to run a seasonal Kendall test, and they estimate the rate of change to be 4.1 μM SO_4/year, equivalent to an almost doubling of the sulfate concentration in ~25 years.

The spatial and temporal variations of the major element concentrations suggest that Cl, SO_4 and Ca in the Min Jiang may have been influenced intensely by human activity while flowing through the Sichuan basin. The source of SO_4 pollution in the Min Jiang is thought to be acid rain from coal burning. According to the Environmental Protection Bureau of Sichuan Province (2002), the Sichuan Basin suffers from acid rain (pH < 5.6), but the eastern Tibet plateau has not been affected. The sulfate concentrations of the Min Jiang tend to be controlled by the acidity and precipitation frequency of the acid rain (Fig. 9). Acid rain also lowers the pH in the river, and the pH at Gaochang station is 0.16~0.35 (average 0.24) units lower than at upstream stations. The pollution sources of Cl in the Min Jiang include Cl_2-treated water for domestic and industrial use in high population centers (Feth, 1971). It is not clear via what route anthropogenic Ca enters the Min Jiang, but calcium carbide (CaC_2), commonly used in chemical factories, could be one source.

5. Conclusion

The headwater and monthly time series samples allow us to examine the dissolved load composition of a major headwater tributary of the Yangtze. The overall major element composition is dominated by carbonate weathering, consistent with the lithology. Both the Si/(Na* + K) ratios of the dissolved load and clay minerals in the bed material indicate that silicate weathering in the watershed is superficial. The concentrations of most elements decrease in response to increasing discharge, with the exception of Ca and Si, which show no apparent trend. TDS and SPM concentrations do not correlate, but their yields are well correlated. Our time series study suggests that the relative uncertainty of the chemical flux calculated using one-time sample in the rising or falling stage is in the range of ±20%. Comparison of the upstream and downstream station data and long-term records at the downstream station imply that SO_4, Cl and Ca are affected by anthropogenic activities. Acid rain, chlorine treatment of water and Ca-rich material used in chemical factories are potential pollution sources.

Acknowledgments

This research was supported in China by the Ministry of Land and Resources and the National Science Foundation and in the United States by National Science Foundation grant OCE-9911416. We thank the two anonymous reviewers for their thoughtful comments and Andre Ellis, Lingling Wu, and Joniell Borges for helpful discussions. **[LW]**

References

Bethke, C.M., 2002. The Geochemist's Workbench 4.0. 224 pp.
Bickle, M.J., Chapman, H.J., Bunbury, J., Harris, N.B.W., Fairchild, I.J., Ahmad, T., Pomiès, C., 2005. Relative contributions of silicate and carbonate rocks to riverine Sr fluxes in the headwaters of the Ganges. Geochim. Cosmochim. Acta 69, 2221–2240.

Bullen, T., White, A., Blum, A., Harden, J., Schulz, M., 1997. Chemical weathering of a soil chronosequence on granitoid alluvium: II. Mineralogic and isotopic constraints on the behavior of strontium. Geochim. Cosmochim. Acta 61, 291–306.

Burchfiel, B.C., Chen, Z., Liu, Y., Royden, L.H., 1995. Tectonics of the Longmen Shan and adjacent regions, Central China. Int. Geol. Rev. 37, 661–735.

Bureau of Geology and Mineral Resources of Sichuan Province, 1991. Regional Geology of Sichuan Province. Geological Publishing House, Beijing. 730 pp. (in Chinese).

Chen, J., Wang, F., Xia, X., Zhang, L., 2002. Major element chemistry of the Changjiang (Yangtze River). Chem. Geol. 187, 231–255.

Chinese Academy of Sciences Comprehensive Research Team, 1985. Hydrologic Geography for the Western Sichuan and Northern Yunnan Area. Science Publishing House, Beijing. 158 pp. (in Chinese).

Clark, M.K., Schoenbohm, L.M., Royden, L.H., Whipple, K.X., Burchfiel, B.C., Zhang, X., Tang, W., Wang, E., Chen, L., 2004. Surface uplift, tectonics, and erosion of eastern Tibet from large-scale drainage patterns. Tectonics 23, doi:10.1029/2002TC001402.

Commission on the Annals of Sichuan Province, 1998. Annals of Sichuan Province (Geology Part). Science and Technological Publishing House of Sichuan Province, Chengdu. 602 pp. (in Chinese).

Edmond, J.M., Huh, Y., 1997. Chemical weathering yields from basement and orogenic terrains in hot and cold climates. In: Ruddiman, W.F. (Ed.), Tectonic Uplift and Climate Change. Plenum Press, pp. 329–351.

Edmond, J.M., Palmer, M.R., Measures, C.I., Grant, B., Stallard, R.F., 1995. The fluvial geochemistry and denudation rate of the Guayana Shield in Venezuela, Colombia and Brazil. Geochim. Cosmochim. Acta 59, 3301–3325.

Environmental Protection Bureau of Sichuan Province, 2002. Report for the Environmental Quality of Sichuan Province in Year 2001, Chengdu. 86 pp. (in Chinese).

Feth, J.H., 1971. Mechanisms controlling world water chemistry. Science 172, 870–872.

Gaillardet, J., Dupré, B., Louvat, P., Allègre, C.J., 1999. Global silicate weathering and CO_2 consumption rates deduced from the chemistry of large rivers. Chem. Geol. 159, 3–30.

Galy, A., France-Lanord, C., 1999. Weathering processes in the Ganges–Brahmaputra basin and the riverine alkalinity budget. Chem. Geol. 159, 31–60.

Hu, M.-H., Stallard, R.F., Edmond, J.M., 1982. Major ion chemistry of some large Chinese rivers. Nature 298, 550–553.

Huh, Y., Tsoi, M.-Y., Zaitsev, A., Edmond, J.M., 1998. The fluvial geochemistry of the rivers of Eastern Siberia: I. Tributaries of the Lena River draining the sedimentary platform of the Siberian Craton. Geochim. Cosmochim. Acta 62, 1657–1676.

Krishnaswami, S., Singh, S.K., Dalai, T.K., 1999. Silicate weathering in the Himalaya: Role in contributing to major ions and radiogenic Sr to the Bay of Bengal. In: Somayajulu, B.L.K. (Ed.), Ocean Science, Trends and Future Directions. Indian National Science Academy and Akademia International, New Delhi, pp. 23-51.

Map Publishing House of China, 1994. Atlas of the Map Plates of the P.R.C. 78 pp. (in Chinese).

Map Publishing House of China, 1998. Atlas of the Chinese Natural Geography Plates, Beijing. 252 pp. (in Chinese).

Meybeck, M., 2003. Global occurrence of major elements in rivers. In: Drever, J.I. (Ed.), Treatise on Geochemistry, Surface and Ground Water, Weathering, and Soils. Elsevier, pp. 207–223.

Millot, R., Gaillardet, J., Dupré, B., Allègre, C.J., 2003. Northern latitude chemical weathering rates: clues from the Mackenzie River Basin, Canada. Geochim. Cosmochim. Acta 67, 1305–1329.

National Soil Survey Office, 1998. The Soil of China. Chinese Agricultural Publishing House, Beijing. 1253 pp. (in Chinese).

Négrel, P., Allègre, C.J., Dupré, B., Lewin, E., 1993. Erosion sources determined by inversion of major and trace element ratios and strontium isotopic ratios in river water: the Congo Basin case. Earth Planet. Sci. Lett. 120, 59–76.

Nkounkou, R.R., Probst, J.L., 1987. Hydrology and geochemistry of the Congo River system. Mitt. Geol.-Paläontol. Inst. Univ. Hamb. 64, S483–S508.

Palmer, M.R., Edmond, J.M., 1989. The strontium isotope budget of the modern ocean. Earth Planet. Sci. Lett. 92, 11–26.

Pan, G.T., Cheng, Z.L., Li, X.Z., Yan, Y.J., Xu, X.S., Xu, Q., Jiang, X.S., Wu, Y.L., Luo, J.L., Zu, T.X., Pen, Y.M., 1997. Geological-Tectonic Evolution in the Eastern Tethys. Geological Publishing House, Beijing. 218 pp. (in Chinese).

Pan, G.T., Li, X.Z., Wang, L.Q., Cheng, Z.L., 2002. Preliminary division of tectonic units of the Qinghai-Tibet Plateau and its adjacent regions. Geol. Bull. China 21, 701–707. (in Chinese).

Raymo, M.E., Ruddiman, W.F., 1992. Tectonic forcing of late Cenozoic climate. Nature 359, 117–122.

Research Center of Tibet Plateau Geology, 2002. Preliminary Study on the Geotectonic Scheme of Tibetan Plateau and its Adjoining Area, Lhasa Meeting for the Tibet Geology. 15 pp. (in Chinese).

Sichuan Head Hydrologic Station, 1984. Minjiang and Tuojiang, Upper Changjiang Hydrologic Information No. 8. Hydrologic Year Book, 6, P.R.C., 569 pp.

Stallard, R.F., Edmond, J.M., 1983. Geochemistry of the Amazon 2. The influence of geology and weathering environment on the dissolved load. J. Geophys. Res. 88, 9671–9688.

West, A.J., Galy, A., Bickle, M., 2005. Tectonic and climatic controls on silicate weathering. Earth Planet. Sci. Lett. 235, 211–228.

Wu, L., Huh, Y., Qin, J., Du, G., Van der Lee, S., in press. Chemical weathering in the Upper Huang He (Yellow River) draining the eastern Qinghai-Tibet Plateau. Geochim. Cosmochim. Acta.

Yoshimura, K., Liu, Z., Cao, J., Yuan, D., Inokura, Y., Noto, M., 2004. Deep source CO_2 in natural waters and its role in extensive tufa deposition in the Huanglong Ravines, Sichuan, China. Chem. Geol. 205, 141–153.

Zhang, J., Huang, W.W., Liu, M.G., Zhou, Q., 1990. Drainage basin weathering and major element transport of two large Chinese rivers (Huanghe and Changjiang). J. Geophys. Res. 95, 13277–13288.

Zhang, D.D., Jim, C.Y., Peart, M.R., Shi, C., 2003. Rapid changes of precipitation of pH in Qinghai Province, the northeastern Tibetan Plateau. Sci. Total Environ. 305, 241–248.